Laser-Stimulated Release of Methylene Blue from Porous Silicon Nanocontainers

Alexandr A. Bubnov[1*], Gleb N. Abrashitov[2], and Victor Yu. Timoshenko[1,2,3]
[1] National Research Nuclear University MEPhI Moscow Engineering Physics Institute Moscow, 31 Kashirskoe str., Moscow 115409, Russian Federation
[2] Lomonosov Moscow State University, GSP-1 Leninskie Gory, Moscow 119991, Russian Federation
[3] P.N. Lebedev Physical Institute, Russian Academy of Sciences, GSP-1, 53 Leninsky Prospekt, Moscow 119991, Russian Federation
*e-mail: bubnov96@mail.ru

Abstract. Aqueous suspensions of nanocontainers consisting of porous silicon (PSi) nanoparticles with Methylene blue (MB) loading were investigated by means of the optical spectroscopy and infrared thermometry under laser irradiation. The photothermal conversion efficiency and kinetics of the MB release from those nanocontainers based on PSi without additional oxidation and after thermal oxidation (ox-PSi) were analyzed to establish an influence of the oxidation of PSi on MB release. The optical spectroscopical study of the loaded nanocontainers showed a strong absorption band of MB at 600−700 nm, while the absorption bands of PSi and, especially, ox-PSi were relatively weak in this spectral region, indicating a high degree of the MB loading for both types of NPs. The MB release from nanocontainers in an aqueous medium was monitored by measuring the MB photoluminescence in the spectral region of 700−800 nm when excited by a continuous wave laser at a wavelength of 660 nm. The MB release from the nanocontainer based on PSi NPs was found to be significantly promoted by nanosecond laser irradiation at 532 nm because of the laser induced heating of PSi NPs. To assess possible applications of the MB release and photoheating, in vitro experiments were carried out with unicellular organisms of Paramecium caudatum, and their results confirmed the effect of spatially localized photoheating of MB-loaded PSi NPs under pulsed laser irradiation, which enhanced the MB release. The obtained results indicate new possibilities for the controlled drug release using PSi NPs and may be useful for biomedical applications as antibacterial treatment and combination therapy of cancer.

Keywords: porous silicon; nanoparticles; nanocontainers; Methylene blue; laser irradiation; photoluminescence; photoheating.

Paper #9129 received 12 Jul 2024; revised manuscript received 4 Sep 2024; accepted for publication 24 Sep 2024; published online 25 Oct 2024. doi: 10.18287/JBPE24.10.040305.

1 Introduction

Nowadays, different types of nanoparticles (NPs) are extensively examined as carriage systems for drug delivery and controlled release in various biomedical applications, e.g. cancer therapy, treatment of cardiovascular diseases, and many others (see for examples [1, 2]). Porous silicon (PSi) NPs are advantageous as a nanocontainer for drugs because they can bind different molecular drugs and at the same time have biodegradability and low toxicity properties [3−6]. While both porous silicon oxide (silica) and PSi can be used for nanocapsulation and delivery of different drugs [1, 2], PSi-based NPs have a significant advantage over porous silica because the formers absorb visible and

near-IR radiations and then they can be directly used as an efficient light absorber for photohyperthermia applications [6]. This property allows us to use PSi NPs as a nanocontainer for the release of a drug triggered by photoheating [7].

Methylene blue (MB) is a dye that absorbs and emits light in the red and near-IR ranges of the spectrum, respectively, and is widely used in medicine for diagnostics and treatment of different diseases [8, 9]. It is worth noting the toxicity of MB when ingested in high concentrations [10, 11]. However, one can use nontoxic NPs as nanocontainers to control the MB concentration in an area of interest in the body. To stimulate the MB release from a nanocontainer the following different stimulus can be applied: laser radiation exposure, oxidation and dialysis [12, 13]. The laser-induced release of nanocapsulated MB can be combined with generation of reactive oxygen species during photoexcitation of MB at 660 nm and it can be used for the photodynamic therapy of cancer [14, 15].

The purpose of this our work was to study nanocontainers made of PSi and thermally oxidized PSi in aqueous suspensions to enhance the controlled release of MB when irradiated with continuous and nanosecond pulsed laser radiation.

2 Materials and Methods

PSi layers were formed by using a procedure of the electrochemical etching (anodization) of boron-doped c-Si wafers with a resistivity of 20 mΩ·cm in HF (48%):C_3H_7OH solution (1:1) at a current density of 50 mA/cm^2 and etching time of 1 h. The procedure allowed us to obtain mesoporous PSi with pore sizes from 2 to 50 nm and mean porosity of about 70%, as determined by using the low-temperature nitrogen sorption analysis and gravimetric measurements, respectively (see for details Refs. [16, 17]). Free-standing PSi films were obtained by applying a short pulse of the anodic current with density of 500 mA/cm^2, followed by rinsing them in deionized water and drying in air. Suspensions of PSi NPs in isopropanol were prepared by high-energy ball-milling of the dried PSi films using a planetary mill with zirconia milling balls. The rotation speed and duration of the milling were 800 rpm and 30 min, respectively. The final concentration of PSi NPs in isopropanol suspension was about 35 mg/mL.

The size and morphology of PSi NPs were analyzed by means of the scanning electron microscopy (SEM) with a Tescan MAIA 3 SEM (Tescan, Czech Republic) apparatus. Fig. 1 shows typical SEM image of PSi NPs. As can be seen from the SEM image, the average size of PSi nanoparticles is of the order of 100 nm, and their shape is irregular due to the mesoporous structure and the mechanical grinding used.

The prepared NP suspension was divided in two parts. The first part was centrifuged in an Eppendorf centrifuge 5804 (10000 rpm, duration 5 min) to remove isopropanol and the resulting precipitate was then mixed with 1 ml of deionized water to produce a concentrated aqueous suspension of PSi NPs. To load MB to the prepared PSi NPs, the corresponding suspension of the latter (0.5 mL, 35 mg/mL) was mixed with an aqueous solution of MB (0.5 mL, 11 mg/mL), followed with stirring for 12 h (rotation speed 110 rpm). The next step was done to separation of the nanocontainers from free MB molecules using centrifugation for 10 min at 10000 rpm, followed by washing the resulting drug-filled nanocontainers with water (1 mL). Due to the high concentration of the resulting suspension, the washing was carried out 3 times. The prepared concentrated suspension of MB-loaded PSi (PSi-MB) nanocontainers were then diluted by deionized water to study the optical and photothermal properties as well the MB release.

The second part of the NP suspension in isopropanol was dried in air at room temperature. After that, the dried PSi NPs were thermally oxidized in an oven at 550 °C for 12 h. Then, the thermally oxidized PSi (ox-PSi) NPs were mixed with distilled water and the obtained suspension was sonicated in an ultrasonic bath for 10 min at room temperature. To load MB into ox-PSi NPs, we applied the above-described procedure of the sorption of MB in a concentrated solution followed by three times rinsing in water, as was used for PSi NPs. The resulting MB-loaded ox-PSi (ox-PSi-MB nanocontainers) were then diluted with water for further analysis and experiments.

Diluted aqueous suspensions of PSi and ox-PSi NPs without loading and MB-loaded were transferred to quartz cuvettes with an optical path length of 10 mm for analysis by means of the optical absorption spectroscopy in the wavelength range from 400 to 900 nm using a UV752P (Wincom Ltd., China) spectrophotometer.

Photoluminescence (PL) of the prepared aqueous suspensions of nanocontainers was measured under excitation by a continuous wave (CW) semiconductor laser with a wavelength of 660 nm. The PL spectra were recorded using a compact Mightex CCD spectrometer equipped with an optical fiber at the input. To suppress the excitation line, a homemade interference filter was used, which was based on a one-dimensional photonic crystal made of a multilayer PSi film (the photonic band gap at 670 nm with a width of about 60 nm), as shown in Fig. 2.

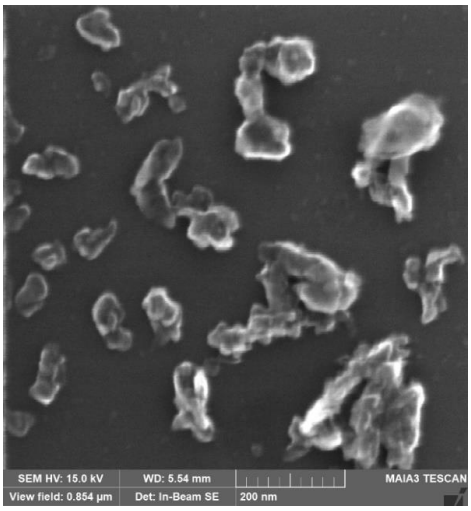

Fig. 1 SEM image of PSi NPs.

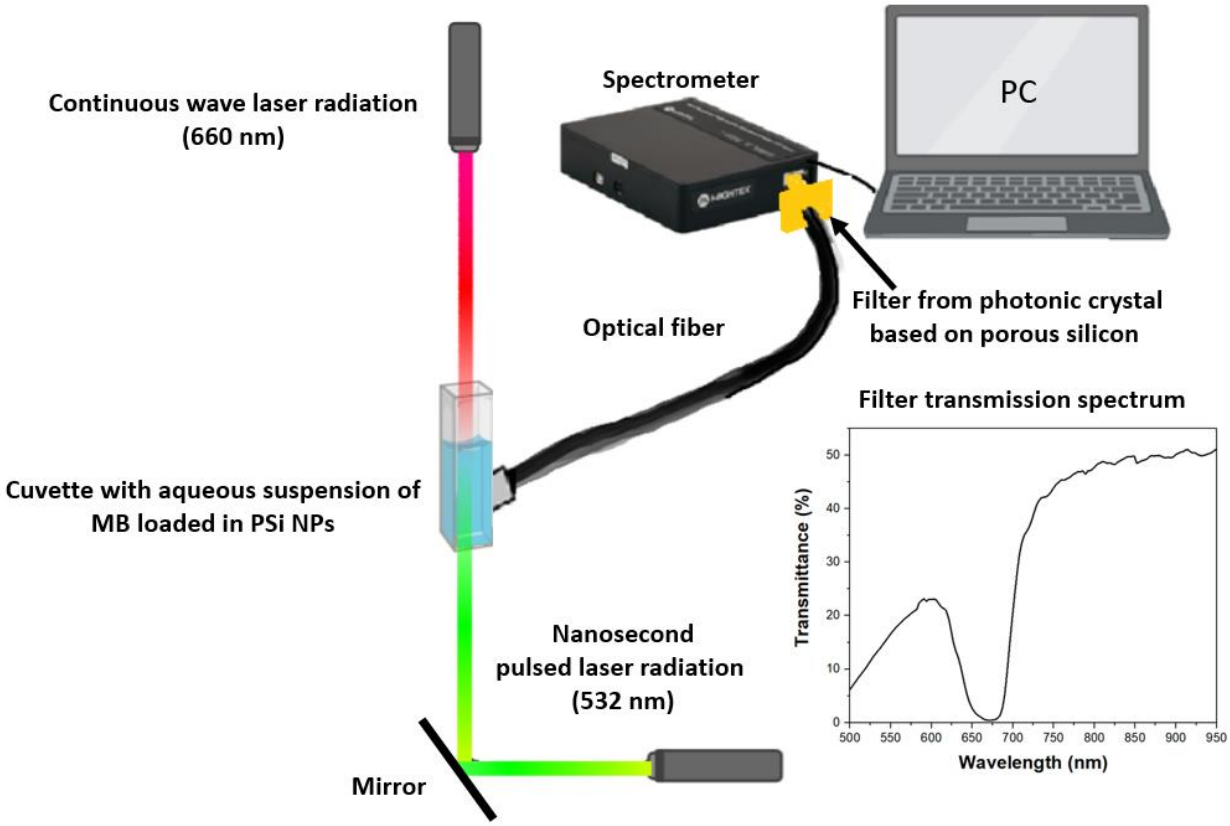

Fig. 2 Schematic representation of the experimental setup for laser irradiation and PL measurements of aqueous suspensions of MB-loaded nanocontainers.

The MB release from PSi nanocontainers was monitored by irradiating the corresponding aqueous suspension (1 mL, 0.1 mg/mL) by a CW laser at 660 nm with the maximal power of about 250 mW under ambient conditions. The collimated laser beam was 4 mm in diameter. The same setup was used for experiments with nanosecond laser irradiation by an AFPL-532-15 diode-pump solid state laser (wavelength of 532 nm, pulse duration of about 15 ns, repetition rate of 4.5 kHz, maximum average power of about 20 mW, laser spot diameter of 2 mm). A schematic representation of the experimental setup is shown in Fig. 2.

Additionally, a thermal imaging camera FLIR C3 with an accuracy of 0.01 °C and sampling rate of 9 Hz was used to monitor temperature of the aqueous suspension of nanocontainers under the influence of laser irradiation.

To assess the biomedical potential of PSi NPs containing MB, we used a model of the unicellular organism *Paramecium caudatum*. The cells were kept in an aqueous solution at a temperature of 24 °C, pH-level of about 7.0 in daylight for 12 h. The cells were fed daily. The last feeding was 2 h before the experiment and was not carried out until the end of the study. Seven groups of cells were used in the experiment (each group with a volume of 1 ml and an average concentration of about 400 cells/mL). The number of cells in each group was determined by analyzing the corresponding video image, while the cell movement was recorded using an Olympus SZ6 binocular stereoscopic microscope. The video was processed by using an open-source Fiji platform with the cell counting plug in Ref. [18]. The main criterion for cell mobility, and therefore their viability, was the average speed of cell movement.

3 Results and Discussion

Fig. 3a shows the extinction spectra of dilute aqueous suspensions of PSi and ox-PSi nanoparticles. The observed monotonic decrease in the extinction with increasing wavelength is explained by the interband absorption of light in silicon (Si) nanocrystals, which are contained in both types of the samples studied [19]. The significantly weaker absorption for the ox-PSi sample compared to the non-oxidized one is obviously due to a large fraction of silicon dioxide, transparent in the visible and near-infrared region, in the first sample.

Fig. 3b shows spectra of the extinction for MB solution as well as for as-prepared suspensions of PSi and ox-PSi NPs loaded with MB. The extinction spectrum of MB consists of two peaks with maxima at ~610 and 664 nm, which are associated with the light absorption by dimeric and monomeric states of MB molecules, respectively [20]. While the spectra for PSi-MB and ox-PSi-MB suspensions are quite similar in the absorption region of MB (550−700 nm), the absorption background for ox-PSi-MB is less pronounced than for the PSi-MB sample. It can be explained by the weaker absorption of ox-PSi NPs compared to the PSi ones.

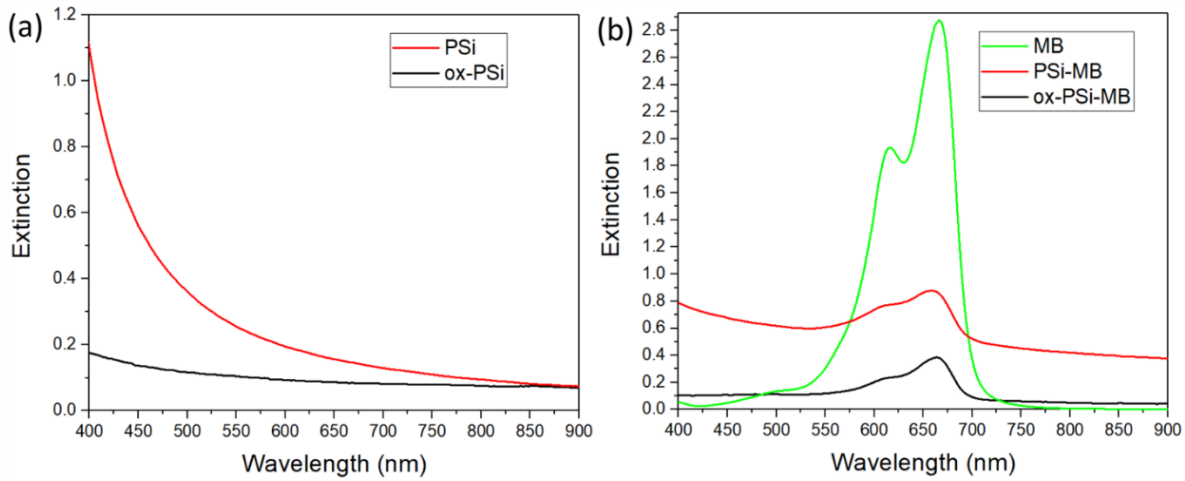

Fig. 3 Extinction spectra of the following samples in aqueous media: (a) suspensions of PSi (red line) and ox-PSi (black line) NPs with concentrations of 0.2 and 0.4 mg/mL, respectively; (b) solution of MB with concentration of 22.6 μM (green line) and as-prepared suspensions of PSi-MB (red line) and ox-PSi-MB (black line) NPs with concentration of 0.1 and 0.02 mg/mL, respectively.

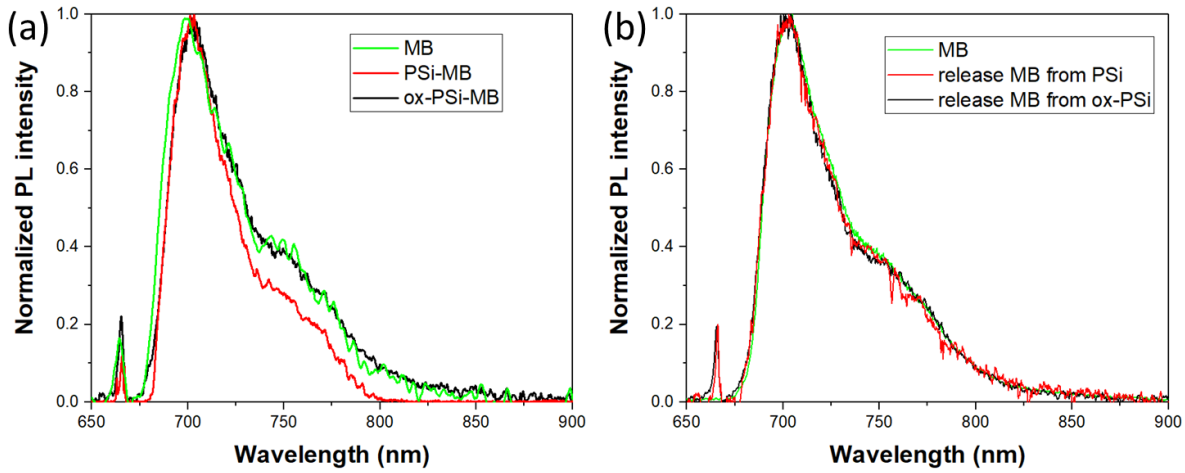

Fig. 4 Normalized PL spectra of the following samples in aqueous media: (a) 0.3 μM MB solution (green line), PSi-MB (red line) and ox-PSi-MB (black line) NP suspensions with concentration of 0.1 and 0.2 mg/mL, respectively; (b) intentionally dissolved MB (green line) and released solutions from PSi-MB (red line) and ox-PSi-MB (black line) NP suspensions. Sharp peaks at a wavelength of 660 nm correspond to the scattered exciting laser radiation, those contribution in the detected signal was suppressed by the used interference filter.

Also, it is worth noting that the extinction spectra of MB-loaded nanocontainer suspensions consist of contributions of both encapsulated and spontaneously released free MB molecules. Since it was difficult to separate these contributions in the total absorption during storage in water for various time scales, we mostly investigated the MB release from nanocontainers by using PL spectroscopy.

Fig. 4a shows the PL spectra of a MB solution and as-prepared aqueous suspensions of PSi-MB and ox-PSi-MB NPs. The spectra consist of a main peak at a wavelength of ~700 and a shoulder at ~750 nm, which are typical for MB solution in water [20]. For the nanocontainers containing MB, a shift of the main peak maximum by about 3 nm towards longer wavelength is observed that can be explained by re-absorption of MB fluorescence due to the elastic light scattering in the NP suspension, as previously reported for suspensions of metal oxide NPs [21, 22]. At the same time, the PL spectra of released MB solutions coincide with the spectrum of free MB molecules in water (Fig. 4b).

To investigate the kinetics of MB release from the NP-based nanocontainers during the CW laser irradiation at 660 nm we analyzed changes in the intensity of MB fluorescence at a wavelength of 700 nm. Fig. 5a shows transients of the normalized change in the PL intensity, which are described by the following Eq.:

$$\Delta I_{PL}(t) = \frac{I_{PL}(t) - I_{PL}(0)}{I_{PL}(0)}, \quad (1)$$

where $I_{PL}(t)$ and $I_{PL}(0)$ are the PL intensities of MB at the analyzed time and at the initial time, respectively.

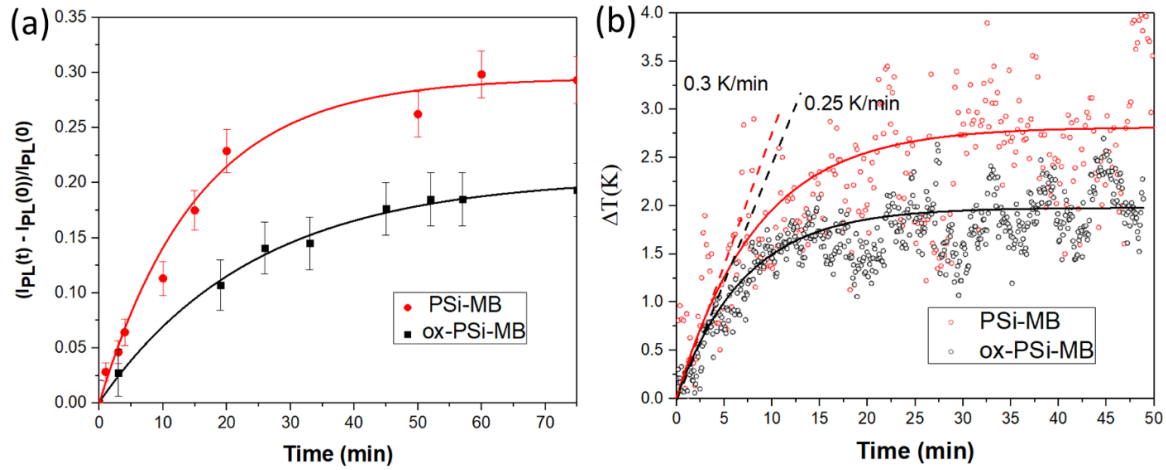

Fig. 5 (a) Transients of the normalized increase of the PL intensity of MB measured at 700 nm for aqueous suspension of PSi-MB (red line) and ox-PSi-MB (black line) nanocontainers with concentration of about 0.5 mg/mL; (b) time dependences of the temperature rise in the same suspension of PSi-MB (red circles) and ox-PSi-MB (black circles) nanocontainers, while the red and black lines are fits by using a solution of the heat balance equation. The CW laser irradiation was done with a wavelength of 660 nm and intensity of 1.2 W/cm^2.

Immediately after the beginning of MB release, the PL intensity transients were well described by the following Eq.:

$$I_{PL}(t) = I_{PL}^{max} \cdot [1 - \exp(-t/\tau)], \qquad (2)$$

where I_{PL}^{max} and τ are the maximal intensity of the MB fluorescence and characteristic time of the release rate, respectively.

As can be seen from Fig. 5a the MB release rate is faster and the relative increase of the PL intensity, i.e. the amount of released MB is larger for PSi-MB NPs, than the corresponding values in the case of ox-PSi-MB. According to the data of PL monitoring shown in Fig. 5a, the total amount of MB release is at about 30 and 18% for nanocontainers from PSi and ox-PSi, respectively. The fact can be associated with stronger binding of MB molecules to the thermally oxidized internal surface of ox-PSi NPs than it is in PSi ones.

It is worth noting that due to the light absorption both in MB and NPs the used CW laser irradiation at 660 nm led to photoheating of the analyzed aqueous media, as shown in Fig. 5b. Differences in maximum heating temperatures indicate different heating rates. By analyzing the temperature rise for the initial stage of photoheating we can evaluate the photoheating conversion efficiency (PCE) with the following Eq. [23]:

$$\eta \approx \frac{C_w \cdot m_w}{I_0 - I_t} \cdot \frac{dT}{dt}, \qquad (3)$$

where I_0 is the incident laser power, I_t is the laser power transmitted through the solution of NPs, m_w and C_w are the mass and specific heat capacity of the photoheated solution, respectively, $\frac{dT}{dt}$ is the initial rate of temperature rise. It should be noted that a more detailed analysis of the thermal balance under continuous laser irradiation gives a temperature rise, which can be fitted by a function like that described by Eq. (2) (see, for example, Ref. [23]).

Using the measured initial photoheating rates (see Fig. 5b) and Eq. (3), the PCE values for PSi-MB and ox-PSi-MB nanocontainers under CW laser excitation at 660 nm are estimated at about 10.4 and 8.5%, respectively. The PCE values for nanocontainers based on PSi and ox-PSi NPs are explained by the strong light absorption by MB, while the contribution of the light absorption by PSi and, especially, ox-PSi are relatively weak at this wavelength (see Fig. 3b). In addition, the same PCE for both types of nanocontainers indicates an almost equally high level of their MB load.

To stimulate release of MB from PSi-MB nanocontainers we have additionally used nanosecond laser irradiation with a wavelength of 532 nm, which was absorbed better in PSi compared to the red light, and the obtained results are shown in Fig. 6. While the CW laser irradiation at 660 nm of PSi-MB suspension led to a steady state level of the PL intensity for the irradiation time of 20−30 min, the additional simultaneous irradiation by nanosecond laser pulses resulted in a significant increase of the MB luminescence intensity and, then, the MB release (Figs. 6 a, b). The effect can be explained by local photoheating of the PSi NPs under the well absorbed pulsed laser radiation, which creates temperature gradients nearby those NPs resulting a stimulus for additional MB release from the pores. The PCE values evaluated from the initial transients of the temperature increase were about 0.22 and 0.42 for the irradiation with the CW laser at 600 nm and pulsed laser at 532 nm, respectively. The PCE increase by 2 times for the latter is obviously related to 2 times stronger absorption of the green light than the red radiation by PSi NPs (see Fig. 2a). Also, it is worth noting that the total temperature increase in the aqueous suspension of nanocontainers after the combined CW and pulsed laser irradiation was about 6.5 °C that was about 2 times larger than for the CW irradiation (Fig. 6c).

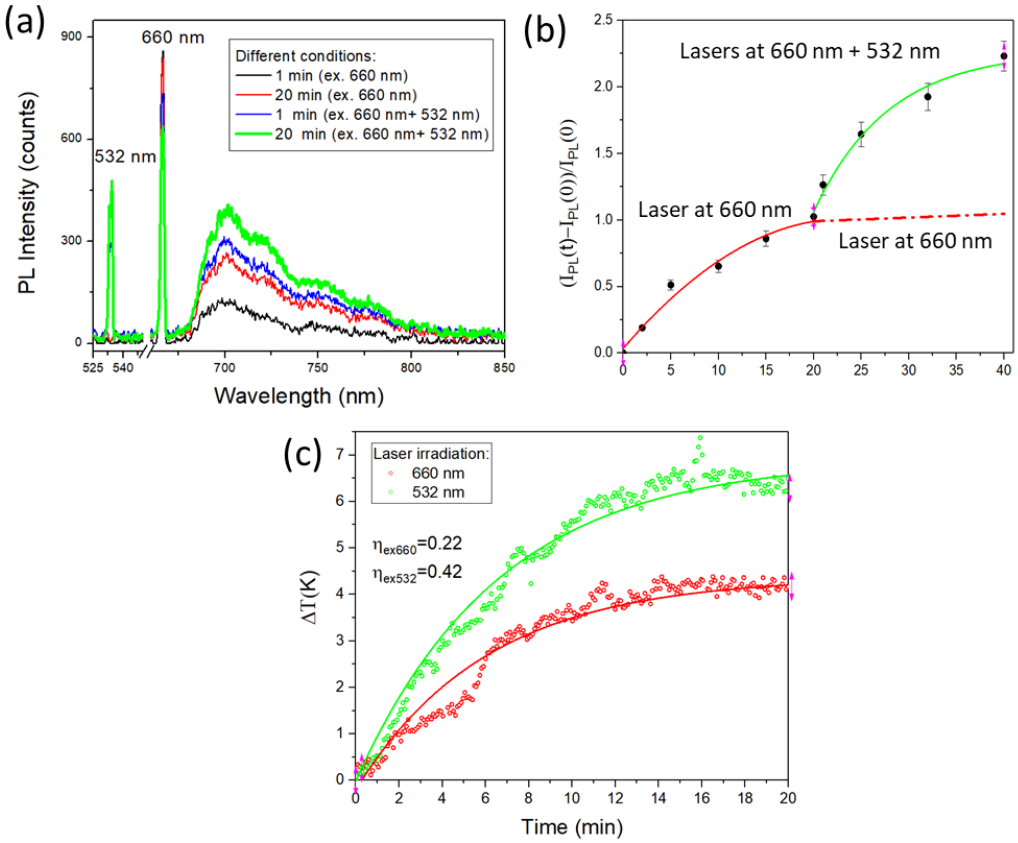

Fig. 6 (a) PL spectra of aqueous suspension of PSi-MB nanocontainers under irradiation by CW laser at 660 nm (black and red lines) followed with additional irradiation with nanosecond pulsed laser at 532 nm (blue and green lines); (b) transients of the normalized increase of the PL intensity of MB at 700 nm under CW laser radiation at 660 nm (red line) followed with simultaneous pulsed laser radiation at 532 nm (green line); (c) time dependences of the temperature increase in aqueous suspension of PSi-MB NPs under CW laser radiation at 660 nm (red circles) and pulsed laser radiation at 532 nm (green circles), while red and green lines are fits by using a solution of the heat balance equation.

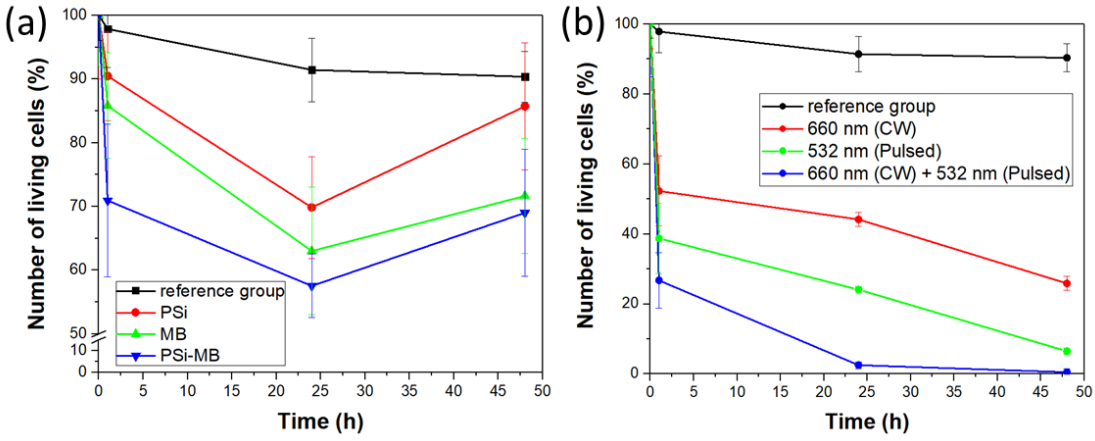

Fig. 7 Time dependences of the relative number of living *Paramecium caudatum* cells for the following groups: (a) reference (black color), PSi NP suspension (red line), MB solution (green line), PSi-MB nanocontainers (blue line); (b) reference (black line), PSi-MB nanocontainers (0.001 mg/mL) under CW laser irradiation at 660 nm (red line), nanosecond pulsed laser radiation at 532 nm (green line) and simultaneous irradiation with CW laser at 660 nm and nanosecond pulsed laser at 532 and (blue line).

The corresponding pulsed photoinduced heating of PSi-MB nanocontainers was obviously even higher that should strongly promote local temperature gradients and thus the MB release under pulsed irradiation at 532 nm.

To assess prospects of a biomedical application of MB-loaded nanocontainers we carried out *in vitro* experiments by using a model of the unicellular organisms *Paramecium caudatum*, which represent

suspension cells sensitive to local hyperthermia and toxic species like cancer cells [24, 25]. This model was previously successfully tested for laser induced photoheating with Si-based NPs [23]. Fig. 7 shows dependence of the cell viability during time after adding PSi NPs, MB solution and PSi-MB nanocontainers without laser irradiation (Fig. 7a) and for cells with added PSi-MB nanocontainers under CW and pulsed laser irradiation (Fig. 7b) as well as for the corresponding reference groups. A decrease in the number of living cells by 25−30% was observed for 24 h after administration of pure PSi NPs. Further, due to cell proliferation, the number of organisms in the suspension was partially restored (see Fig. 7a). The observed toxicity of PSi NPs was significantly lower than that for PSi-MB nanocontainers (blue curve in Fig. 7a), while free MB solution with the same MB concentration led to the similar toxic effect (green curve in Fig. 7a).

Fig. 7b shows a sharp decrease in the number of living cells during one hour just after laser irradiation for all groups. The effect was especially pronounced after the simultaneous irradiation by CW and nanosecond lasers. In this case, the cell viability during the first hour was only about 20%. In addition, the number of living cells was 2−3% within 24 h after irradiation and decreased to almost zero the next day. If the sample was only irradiated by CW laser at 660 nm it was observed a sharp decrease of the number of living cells by 50% and the further rate of cell loss slowed down. The decrease in the rate of cell death could be due to the competing process of cell proliferation.

4 Conclusions

The optical and photothermal properties of nanocontainers based on PSi NPs filled with MB molecules were studied and the obtained results showed the influence of the oxide fraction in PSi NPs as well the role of pulsed laser irradiation on the MB release. It has been established the values of PCE under CW laser irradiation at 660 nm were quite similar for PSi NPs without special oxidation and for ox-PSi NPs obtained after additional thermal oxidation at 550 °C. Despite of this, the MB release was almost two times better from the PSi-MB NPs than that from ox-PSi-MB ones. The fact can be explained by stronger binding of MB molecules with the surface of thermally oxidized PSi NPs. To increase further the MB release from PSi-MB NPs the nanosecond pulsed laser irradiation at 532 nm was rather efficient. The estimated enhancement of the MB release was about 2.3 times compared to the case of CW irradiation by the laser at 600 nm. This enhancement can be explained by local photoheating of PSi NPs by nanosecond laser pulses that induces local temperature gradients nearby those NPs, which promote the MB release from their pores. Also, the PCE value of MB-loaded PSi NPs under laser radiation at 532 nm was found to be larger by 2 times compared to the CW laser irradiation at 660 nm. Therefore, the pulsed laser induced photoheating can be efficiently combined with MB release from PSi-based nanocontainers. The combine effect of the photoheating and MB release was checked out by using in vitro experiment with unicellular organisms *Paramecium caudatum*. The pulsed laser irradiation of the cells with added PSi-MB nanocontainers resulted in almost complete cell death. This fact is explained by considering the laser stimulated MB release from PSi NPs due to their photoheating, which leads to the spatial-localized photohyperthermia combined with increased MB concentration. The obtained results indicate that PSi NPs can be considered as promising nanocontainers for MB with possibility to control the drug realize by using additional oxidation of PSi NPs as well the pulsed laser irradiation as an external stimulus.

Acknowledgements

The authors acknowledge Dr. A. Yu. Kharin and Ms. A. S. Eremina for the assistance with SEM measurements and sample preparation, respectively. The work was partially supported by the grant FSWU-2023-0070 of Ministry of Science and Higher Education of the Russian Federation.

Disclosures

The authors declare that they have no conflict of interest.

Data Availability Statement

The data presented in this study are available on request from the corresponding author.

References

1. O. Afzal, A. S. A. Altamimi, M. S. Nadeem, S. I. Alzarea, W. H. Almalki, A. Tariq, B. Mubeen, B. N. Murtaza, S. Iftikhar, N. Riaz, and I. Kazmi, "Nanoparticles in Drug Delivery: From History to Therapeutic Applications," Nanomaterials 12(24), 4494 (2022).
2. A. Yusuf, A. R. Z. Almotairy, H. Henidi, O. Y. Alshehri, and M. S. Aldughaim, "Nanoparticles as Drug Delivery Systems: A Review of the Implication of Nanoparticles' Physicochemical Properties on Responses in Biological Systems," Polymers 15(7), 1596 (2023).
3. J.-H. Park, L. Gu, G. Von Maltzahn, E. Ruoslahti, S. N. Bhatia, and M. J. Sailor, "Biodegradable luminescent porous silicon nanoparticles for in vivo applications," Nature Mater 8(4), 331–336 (2009).

4. S. M.Haidary, E. P.Córcoles, and N. K. Ali, "Nanoporous Silicon as Drug Delivery Systems for Cancer Therapies," Journal of Nanomaterials 2012(1), 830503 (2012).
5. J. Salonen, "Drug delivery with porous silicon," in Handbook of Porous Silicon, L. Canham (Ed.), 2 ed., Springer, Cham, 1377–1390 (2018). Online ISBN: 978-3-319-71381-6.
6. V. Yu. Timoshenko, "Porous silicon in photodynamic and photothermal therapy," in Handbook of Porous Silicon, L. Canham (Ed.), 2 ed., Springer, Cham, 1461−1469 (2018).
7. K. Tamarov, W. Xu, L. Osminkina, S. Zinovyev, P. Soininen, A. Kudryavtsev, M. Gongalsky, A. Gaydarova, A. Närvänen, V. Timoshenko, and V.-P. Lehto, "Temperature responsive porous silicon nanoparticles for cancer therapy – spatiotemporal triggering through infrared and radiofrequency electromagnetic heating," Journal of Controlled Release 241, 220−228 (2016).
8. T. Cwalinski, W. Polom, L. Marano, G. Roviello, A. D'Angelo, N. Cwalina, M. Matuszewski, F. Roviello, J. Jaskiewicz, and K. Polom, "Methylene blue-current knowledge, fluorescent properties, and its future use," Journal of Clinical Medicine 9(11), 3538 (2020).
9. L. Abraham, A. Rai, K. Burde, and V. Naikmasur, "Methylene blue as a diagnostic aid in the early detection of potentially malignant and malignant lesions of oral Mucosa," Ethiopian Journal of Health Sciences 26(3), 201−208 (2016).
10. M. Bužga, E. Machytka, E. Dvořáčková, Z. Švagera, D. Stejskal, J. Máca, and J. Král, "Methylene blue: a controversial diagnostic acid and medication?," Toxicology Research 11(5), 711−717 (2022).
11. S. Li, Y. Cui, M. Wen, and G. Ji, "Toxic effects of Methylene blue on the growth, reproduction and physiology of Daphnia magna," Toxics 11(7), 594 (2023).
12. A. S. Altowyan, A. Toghan, H. A. Ahmed, R. A. Pashameah, E. A. Mwafy, S. H. Alrefaee, and A. M. Mostafa, "Removal of methylene blue dye from aqueous solution using carbon nanotubes decorated by nickel oxide nanoparticles via pulsed laser ablation method," Radiation Physics and Chemistry 198, 110268 (2022).
13. M. Chen, C. T. Jafvert, "Application of cross-linked stearic acid nanoparticles with dialysis membranes for methylene blue recovery," Separation and Purification Technology 204, 21−29 (2018).
14. W. Tang, H. Xu, R. Kopelman and M. A. Philbert, "Photodynamic characterization and in vitro application of methylene blue-containing nanoparticle platforms," Photochemistry and Photobiology 81(2), 242–249 (2005).
15. X. Xu, H. Mao, Y. Wu, S. Liu, J. Liu, Q. Li, M. Yang, J. Zhu, S. Zou, and F. Du, "Fabrication of methylene blue-loaded ovalbumin/polypyrrole nanoparticles for enhanced phototherapy-triggered antitumour immune activation," Journal of Nanobiotechnology 20, 297 (2022).
16. M. A. Konoplyannikov, A. S. Eremina, Yu. V. Kargina, I. M. Le-Deygen, A. Yu. Kharin, T. Yu. Bazylenko, G. M. Yusubalieva, V. A. Revkova, O. N. Matchuk, I. A. Zamulaeva, M. R. Abramova, S. L. Kotova, P. S. Timashev, V. P. Baklaushev, and V. Yu. Timoshenko, "Mesoporous silicon nanoparticles loaded with salinomycin for cancer therapy applications," Microporous and Mesoporous Materials 328, 111473 (2021).
17. A. S. Eremina, Yu. V. Kargina, A. Yu. Kharin, D. I. Petukhov, and V. Yu. Timoshenko, "Mesoporous silicon nanoparticles covered with PEG molecules by mechanical grinding in aqueous suspensions," Microporous and Mesoporous Materials 331, 111641 (2022).
18. J. Schindelin, I. Arganda-Carreras, E. Frise, V. Kaynig, M. Longair, T. Pietzsch, S. Preibisch, C. Rueden, S. Saalfeld, B. Schmid, J.-Y. Tinevez, D. J. White, V. Hartenstein, K. Eliceiri, P. Tomancak, and A. Cardona, "Fiji: an open-source platform for biological-image analysis," Nature Methods 9(7), 676–682 (2012).
19. D. Kovalev, H. Heckler, G. Polisski, and F. Koch, "Optical properties of Si nanocrystals", Physica Status Solidi (B) 215(2), 871–932 (1999).
20. É. G. A. De Miranda, V. H. Toledo, C. G. Dos Santos, F. Costa, M. Diaz-Lopez, T. B. De Queiroz, O. R. Nascimento, and I. L. Nantes, "Organic matrix-entrapped methylene blue as a photochemical reactor applied in chemical synthesis and nanotechnology," Journal of Photochemistry and Photobiology A: Chemistry 444, 115015 (2023).
21. H. M. Dao, C. Whang, V. K. Shankar, Y. Wang, I. A. Khan, L. A. Walker, I. Husain, S. I. Khan, S. N. Murthy and S. Jo, "Methylene blue as a far-red light-mediated photocleavable multifunctional ligand," Chemical Communications 56(11), 1673−1676 (2020).
22. F. Pahang, P. Parvin, H. Ghafoori-Fard, A. Bavali, and A. Moafi, "Fluorescence properties of methylene blue molecules coupled with metal oxide nanoparticles," OSA Continuum 3(3), 688−697 (2020).
23. A. A. Bubnov, V. S. Belov, Y. V. Kargina, G. V. Tikhonowski, A. A. Popov, A. Yu. Kharin, M. V. Shestakov, A. M. Perepukhov, A. V. Syuy, V. S. Volkov, V. V. Khovaylo, S. M. Klimentov, A. V. Kabashin, and V. Yu. Timoshenko, "Laser-Ablative Synthesis of Silicon–Iron Composite Nanoparticles for Theranostic Applications," Nanomaterials 13(15), 2256 (2023).
24. S. Krenek, T. U. Berendonk, and T. Petzoldt, "Thermal performance curves of Paramecium caudatum: A model selection approach," European Journal of Protistology 47(2), 124–137 (2011).
25. G. A. Gruzdev, O. V. Karpukhina, V. G. Yakunin, A. N. Inozemtsev, V. P. Savinov, V. Yu. Timoshenko, and A. A. Kamensky, "Effect of Low-Temperature Atmospheric Pressure Plasma on Paramecium caudatum Cell Culture," Moscow University Biological Sciences Bulletin 76(4), 244–248 (2021).